A Novel Single-Switch Cascaded DC-DC Converter of Boost and Buck-Boost Converters

Jian Fu; Bo Zhang; Dongyuan Qiu; Wenxun Xiao
School of Electric Power
South China University of Technology
Guangzhou, China
Email: epbzhang@scut.edu.cn

Acknowledgements

This work was supported in part by the Key Program of the National Natural Science Foundation of China under Grant 50937001, and by Guangdong strategic emerging industry special fund project under Grant 2010A081002004.

Keywords

«Single-switch», «Cascaded converter», «DC-DC converter», «Boost converter», «Buck-boost converter»

Abstract

This paper proposes a novel single-switch dc-dc converter with voltage gain $D/(1-D)^2$ by cascading a Boost converter and a Buck-boost converter. The proposed converter has the advantages of simple circuit structure and extended voltage conversion ratio. The operating principle and steady-state analysis of the proposed converter are discussed in detail. Finally, a prototype is implemented to verify theoretical analysis.

Introduction

In recent year, high voltage gain dc-dc converters play more and more important role in many industry applications such as uninterrupted power supplies, power factor correctors, distributed photovoltaic (PV) generation systems and fuel cell energy conversion systems [1-10]. In these applications, a classical boost converter is normally used, but the extremely high duty cycle will result in large conduction loss on the power devices and serious reverse recovery problems [11]. Thus, the conventional boost converter would not be acceptable for realizing high step-up voltage gain along with high efficiency.

To achieve a high conversion ratio without operating at extremely high duty ratio, some converters based on transformers or coupled inductors or tapped inductors have been provided [12-15]. However, the leakage inductance in the transformer, coupled inductor or tapped inductor will cause high voltage spikes in the switches and reduce system efficiency. In order to solve the voltage spike, snubber circuits, such as resistor–capacitor–diode snubber, nondissipative snubber and active clamp circuit, can be applied, but increase the complexity of converter structure.

Some nonisolated topologies have been proposed to achieve a high conversion ratio and avoid operating at extremely high-duty cycle. These converters include the switched-capacitor type [16], switched-inductor type [17], the voltage-doubler circuit [18], and the capacitor-diode voltage multiplier [19]. All of them can obtain higher voltage gain than the conventional boost converter. However, more switched capacitor or switched-inductor stages are needed for an extremely large conversion ratio, which result in higher cost and complex circuit.

The voltage gain can be extended to satisfy the high-step-up requirements by employing the cascade structure. A cascaded boost converter with two stages was proposed in [20]. However, the cascade converter requires two sets of power devices and control circuits, which is complex and expensive. The two switches in the cascade boost converter can be integrated into one switch to reduce circuit complexity [21]. Furthermore, [22] proposed three single-switch cascaded converters, including quadratic buck converter, quadratic buck-boost converter, and buck-buck-boost converter, whose voltage gain is D^2, $D^2/(1-D)^2$ and $D^2/(1-D)$, respectively.

A novel single-switch cascaded dc-dc converter of boost and buck-boost converts is proposed in this paper. The voltage conversion ratio is extended to $D/(1-D)^2$. The proposed converter operates as basic boost and buck-boost converters in cascade. The features of the proposed converter are as follows: 1) the voltage gain is increased by operating as basic boost and buck-boost converters in cascade, compared with classical dc-dc converters; 2) only one switch is used to realize cascaded converter of basic boost and buck-boost converters, which efficiently simplify the circuit structure; 3) the number of magnetic components is small, where only two inductors are used just like Cuk and Sepic converter.

Operating principle of the proposed converter in steady-state is given firstly. Secondly, the circuit performance is analyzed, while the static voltage gain is derived. Next, the experimental results are provided to verify the analysis. A valuable summary is made in final.

Operating principle of the proposed converter

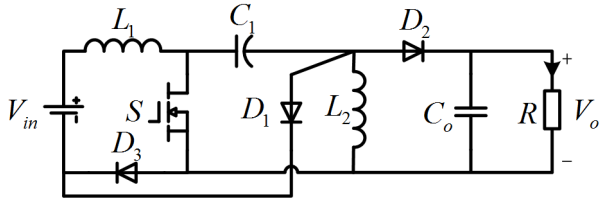

Fig. 1 The proposed single-switch cascaded converter

Fig. 1 shows the circuit structure of the proposed converter, which consists of an active switch S, diodes D_1, D_2 and D_3, an input inductor L_1, an output inductor L_2, a storage energy capacitor C_1 and an output capacitor C_o.

The input inductance L_1 is assumed to be large enough so that input current i_{L1} is continuous. Capacitors C_1 and C_o are sufficiently large, and the voltages across them are considered constant during one switching period.

When the inductor current i_{L2} is in continuous conduction mode, L_2-CCM is used to denote the operating mode; and L_2-DCM stands for the mode in which i_{L2} is in discontinuous conduction mode.

A. L_2-CCM

Based on the aforementioned assumption, Fig. 2(a) illustrates some key waveforms under L_2-CCM, and the corresponding equivalent circuits are shown in Fig. 3(a) and (b). The operating stages are described as follows.

Mode I [t_0-t_1]: Switch S conducts at $t=t_0$. Diodes D_1 and D_2 are reverse-biased by V_{C1} and $V_{C1}+V_o$, respectively. Only diode D_3 is ON. Fig. 3(a) shows the current-flow path. The energy of dc source V_{in} is transferred to the inductor L_1 through S and D_3. Therefore, inductor current i_{L1} is increasing linearly. The voltage of the inductor L_2 is V_{C1} and the capacitor C_1 is discharging its energy to L_2 though S. The inductor current i_{L2} is increasing. Meanwhile, the load R is supplied by the output capacitor C_o. This stage ends at $t=t_1$.

Mode II [t_1-t_2]: Fig. 3(b) depicts the current-flow path of this stage. Once S is turned OFF at $t=t_1$, i_{L1} is forced to flow through D_1, inductor L_1 and dc source V_{in} charge capacitor C_1 instantaneously.

Therefore, i_{L1} declines linearly. At the same time, i_{L2} is forced to flow through D_2 and the energy stored in inductor L_2 is transferred to the output capacitor C_o and load R. Thus, i_{L2} declines linearly and D_3 is reverse-biased by V_{in}. This stage end at $t=t_2$.

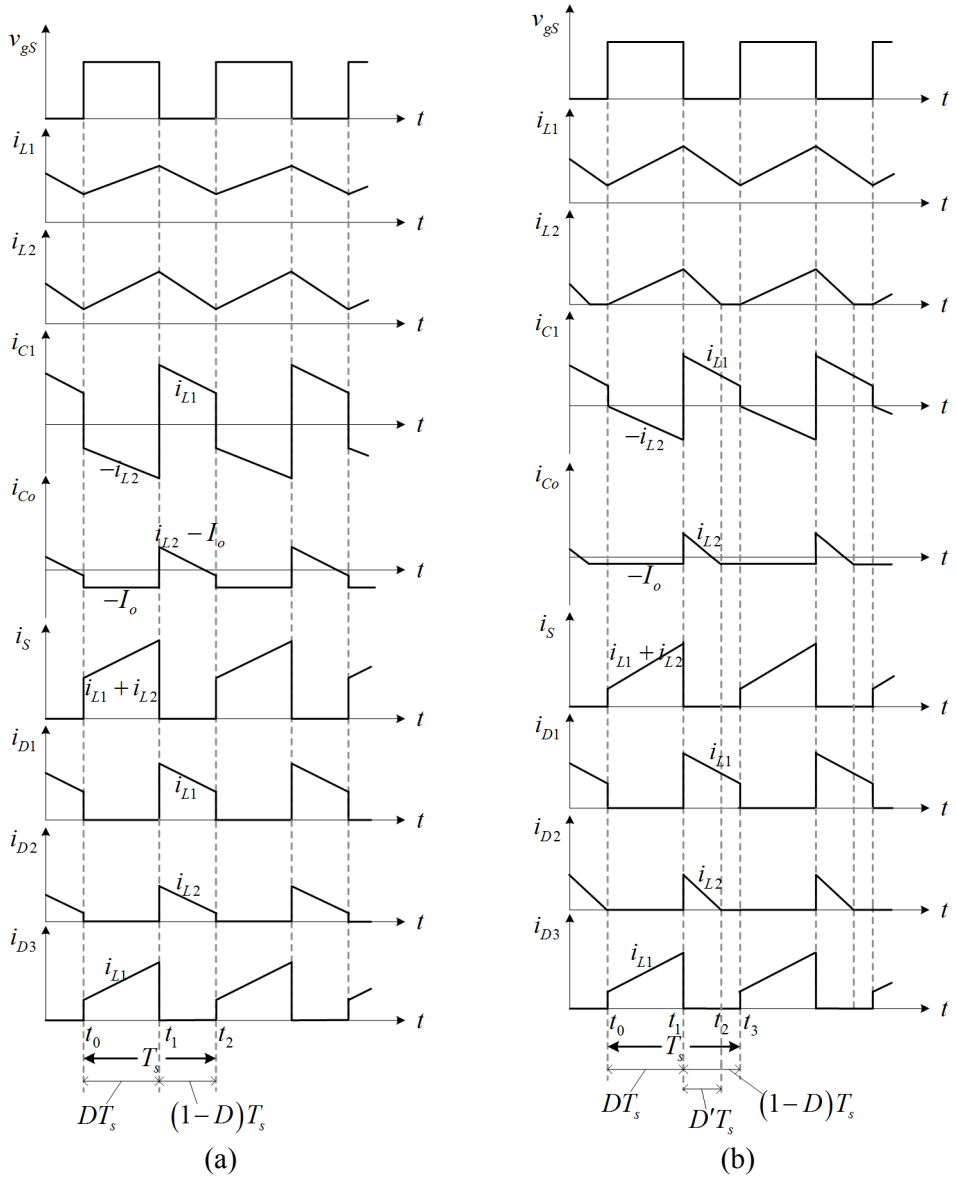

Fig. 2 Key waveforms of the proposed converter: (a) L_2-CCM operation; (b) L_2-DCM operation

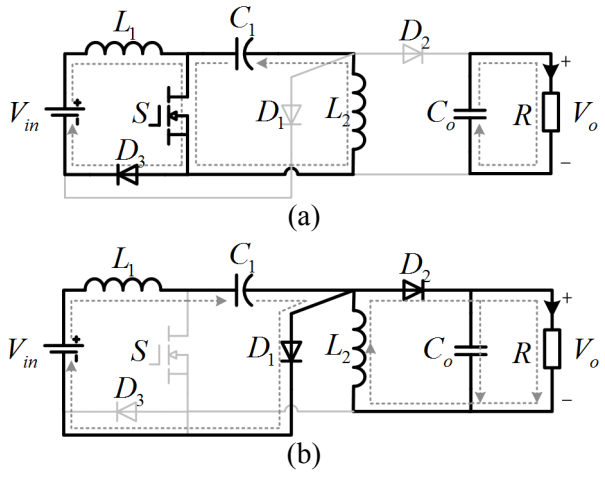

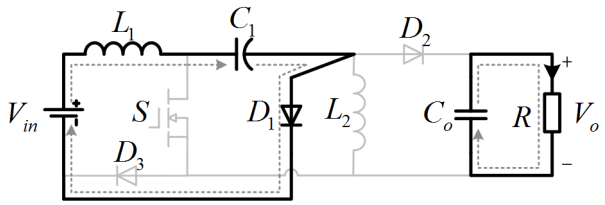

(c)

Fig. 3 Equivalent circuits of operating stages: (a) Mode I; (b) Mode II; (c) Mode III.

B. L_2-DCM

The key waveforms of the proposed converter under L_2-DCM are shown in Fig. 2(b). There are three main stages during one switching cycle. The equivalent circuits for each subinterval are shown in Fig. 3(a), (b) and (c). Modes I and II are same with L_2-CCM, and only case III is presented.

Mode III [t_2-t_3]: Diode D_2 is blocked when the current i_{L2} reaches zero at t=t_2. During this time interval, switch S and diodes D_2, D_3 are turned OFF, only diode D_1 is turned ON. The current path is shown in Fig. 3(c). The dc source V_{in} is in series with inductor L_1 and keeps transferring energy to the capacitor C_1 through D_1. Since the energy stored in L_2 is empty, the energy stored in C_o is discharged to load R. This stage ends when switch S is turned ON at t=t_3, the next switching period will begin again.

Steady-state analysis of the proposed converter

To simplify the analysis, all components are considered to be ideal, and the losses of the power devices are not considered.

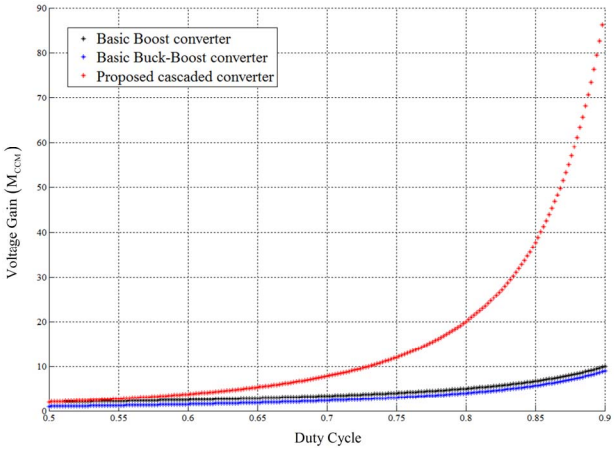

Fig. 4: Voltage gain comparison of the proposed converter, Boost converter and Buck-Boost converter

A. L_2-CCM

Using the inductor volt-second balance principle to the inductors L_1 and L_2, the following equations can be established.

$$\int_0^{DT_s} V_{in}\,dt + \int_{DT_s}^{T_s} \left(V_{in} - V_{C1}\right) dt = 0 \tag{1}$$

$$\int_0^{DT_s} V_{C1}\,dt + \int_{DT_s}^{T_s} \left(-V_o\right) dt = 0 \tag{2}$$

Then, the dc voltage gain M_{CCM} is obtained as

$$M_{CCM} = \frac{V_o}{V_{in}} = \frac{D}{(1-D)^2} \tag{3}$$

Fig. 4 demonstrates the relationships between the voltage gain and the duty cycle in the basic boost converter, buck-boost converter, and the proposed converter under L_2-CCM. It is found that the proposed converter can realize higher voltage gain with the same duty cycle.

B. L_2-DCM

If *D'* is defined as the duty cycle of the inductor current i_{L2} from peak point down to zero. By applying the volt-second balance principle to the inductors L_1 and L_2, the following equations are derived.

$$\int_0^{DT_s} V_{in}\,dt + \int_{DT_s}^{T_s} (V_{in} - V_{C1})\,dt = 0 \tag{4}$$

$$\int_0^{DT_s} V_{C1}\,dt + \int_{DT_s}^{(D+D')T_s} (-V_o)\,dt = 0 \tag{5}$$

Then, the voltage gain are obtained

$$M_{DCM} = \frac{V_o}{V_{in}} = \frac{D}{(1-D)D'} \tag{6}$$

The currents flow capacitor C_o at mode I, II, and III are $-I_o$, $i_{L2}-I_o$ and $-I_o$, respectively. According to the current-balance principle on capacitor C_o, the following equation can be established.

$$\int_0^{DT_s} (-I_o)\,dt + \int_{DT_s}^{(D+D')T_s} (i_{L2} - I_o)\,dt + \int_{(D+D')T_s}^{T_s} (-I_o)\,dt = 0 \tag{7}$$

Since $I_o=V_o/R_L$, the following relationship can be obtained.

$$D'^2 + \frac{2L_2 f_s}{R} D' - \frac{2L_2 f_s}{R} = 0 \tag{8}$$

where f_s is the switching frequency.

C. Boundary condition between L_2-CCM and L_2-DCM

If the proposed converter is operating in boundary condition mode (BCM) between L2-CCM and L2-DCM, the peak value of the inductor current i_{L2} is given as

$$I_{L2p} = \frac{V_{C1}}{L_2} DT_S \tag{9}$$

The currents flow capacitor C_o at mode I and II are $-I_o$ and $i_{L2}-I_o$, respectively. According to the current-balance principle on capacitor C_o, the following equation can be established.

$$\int_0^{DT_s} (-I_o)\,dt + \int_{DT_s}^{T_s} (i_{L2} - I_o)\,dt = 0 \tag{10}$$

Thus

$$\frac{1}{2} I_{L2p} (1-D) = I_o \tag{11}$$

The normalized inductor time constant τ_{L2} is defined as

$$\tau_{L2} \equiv \frac{L_2 f_s}{R_L} \tag{12}$$

Since $I_o=V_o/R_L$, by substituting (4), (9) and (12) into (11), the boundary normalized inductor time constant τ_{L2B} is obtained, which is

$$\tau_{L2B} = \frac{(1-D)^2}{2} \tag{13}$$

Based on (13), the relationship between τ_{L2B} and duty cycle D is plotted in Fig. 5. Once the τ_{L2} is higher than τ_{L2B}, the proposed converter is operating in L_2-CCM, but in L_2-DCM when the τ_{L2} is lower than τ_{L2B}.

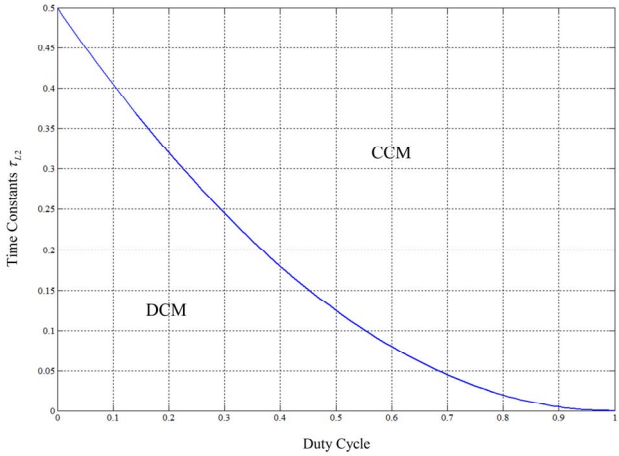

Fig. 5 The boundary condition of the proposed converter

Experimental Results

To demonstrate the effectiveness of the theoretical analysis, a prototype of the proposed converter was built and tested. The test setup is shown in Fig. 6 and the components used in the prototype are listed in Table I. A PWM signal with fixed duty ratio is generated to control the switch on or off.

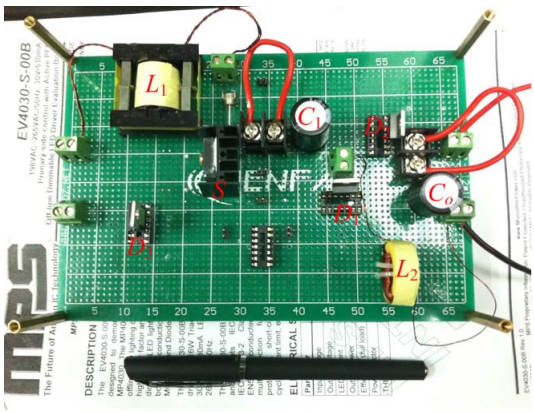

Fig. 6 The prototype of the proposed converter.

Table I Utilized Components and Parameters of Prototype

Components	Parameters	Components	Parameters
Output power P_o	36W	Output Inductor L_2	150uH
Input voltage V_{in}	10V	Capacitor C_1	470uF
Output voltage V_o	60V	Output capacitor C_o	100uF
Switching frequency f_s	50kHz	Power MOSFET S	STW15NA50
Input inductor L_1	400uH	Diodes $D_1/D_2/D_3$	BYV34

Typical waveforms in L_2-CCM are demonstrated in Fig. 7. Fig. 7(a) illustrates the gate signal of switch (v_{gS}), the voltage across C_1, and the output voltage V_o. Fig. 7(b) illustrates v_{gS} and the voltage of switch S, and the output voltage V_o. Fig. 7(c) shows v_{gS} and inductor currents i_{L1} and i_{L2}. Fig. 7(d) gives v_{gS} and capacitor currents i_{C1} and i_{Co}, which are agreed well with the theoretical analysis.

In order to verify the feasibility of L_2-DCM, the experimental waveforms under light-load are shown in Fig. 8. The inductor current i_{L2} declines to zero during the off state of switch S. The experimental results are consistent with the theoretical analysis as well.

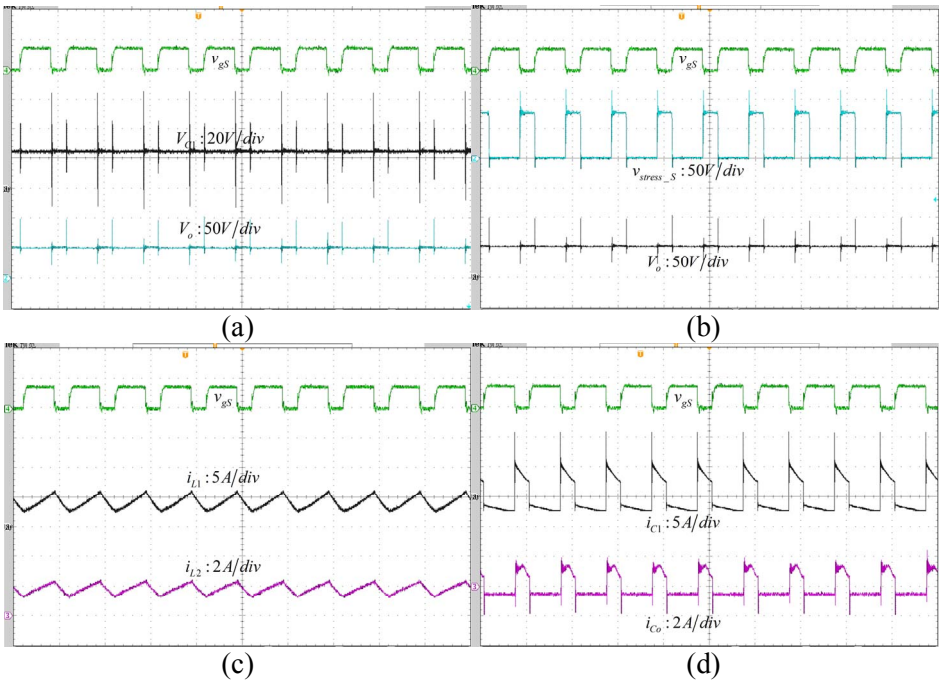

Fig. 7 Experimental waveforms under L_2-CCM: (a) v_{gS}, v_{C1}, V_o. (b) v_{gS}, v_S, V_o; (c) v_{gS}, i_{L1}, i_{L2}; (d) v_{gS}, i_{C1}, i_{Co}.

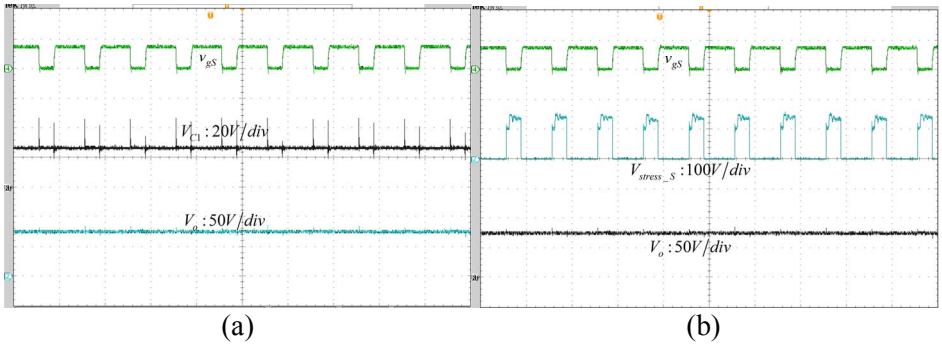

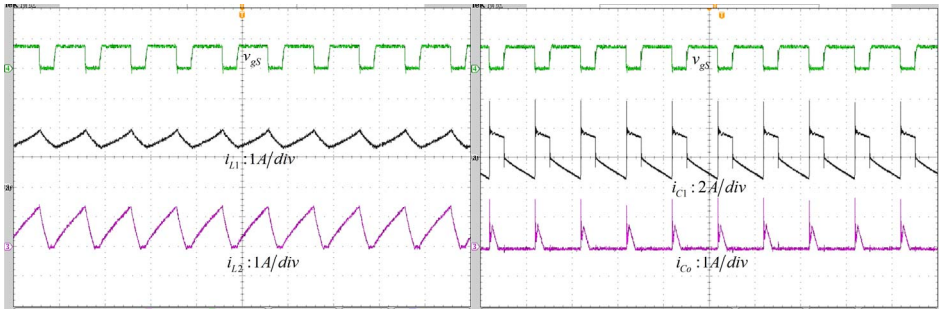

(c) (d)

Fig. 8 Experimental waveforms under L_2-DCM: (a) v_{gS}, v_{C1}, V_o; (b) v_{gS}, v_S, V_o; (c) v_{gS}, i_{L1}, i_{L2}; (d) v_{gS}, i_{C1}, i_{Co}.

Conclusion

A novel single-switch cascaded converter is proposed in this paper. Only single switch is used to realize the cascaded converter of basic boost and buck-boost converters. The voltage conversion ratio is extended to $D/(1-D)^2$. The proposed converter operates as basic boost and buck-boost converters in cascade, which has simple circuit structure with extended voltage conversion ratio compared with some other high step-up converters. The number of magnetic components is reduced, where only two inductors are used just like Cuk and Sepic converters, results in lower cost and simple circuit.

References

[1] J F. Boico, B. Lehman, and K. Shujaee, "Solar battery chargers for NiMH batteries," IEEE Trans. Power Electron., vol. 26, no. 5, pp. 1600–1609, Sep. 2007

[2] P. F. de Melo, R. Gules, E. F. R. Romaneli, and R. C. Annunziato, "A modified SEPIC converter for high power factor rectifier and universal input voltage applications," IEEE Trans. Power Electron., vol. 25, no. 2, Feb. 2010

[3] Vaccaro, G. Velotto, and A. F. Zobaa, "A decentralized and cooperative architecture for optimal voltage regulation in smart grids," IEEE Trans. Ind. Electron., vol. 58, no. 10, pp. 4593–4602, Oct. 2011

[4] Q Li and P Wolfs, "A review of the single phase photovoltaic module integrated converter topologies with three different DC link configurations," IEEE Trans. Power Electron., vol. 23, no. 3, pp. 1320–1333, May 2008

[5] H. S. H. Chung, W. C. Chow, S. Y. R. Hui, and S. T. S. Lee, "Development of a switched-capacitor DC–DC converter with bidirectional power flow," IEEE Trans. Circuits Syst. I, Fund. Theory Appl., vol. 47, no. 9, pp. 1383–1389, Sep. 2000

[6] E. K. Sato, M. Kinoshita, Y. Yamamoto, and T. Amboh, "Redundant high density high-efficiency double-conversion uninterruptible power system," IEEE Trans. Ind. Appl., vol. 46, no. 4, pp. 1525–1533, Jul./Aug. 2010

[7] S. V. Araujo, R. P. Torrico-Bascope, and G. V. Torrico-Bascope, "Highly efficient high step-up converter for fuel-cell power processing based on three-state commutation cell," IEEE Trans. Ind. Electron., vol. 57, no. 6, pp. 1987–1997, Jun. 2010

[8] Z. Amjadi and S. S. Williamson, "Power electronics based solutions for plug-in hybrid electric vehicle energy storage and management systems," IEEE Trans. Ind. Electron., vol. 57, no. 2, pp. 608–616, Feb. 2010

[9] R. A. da Camara, C. M. T. Cruz, and R. P. Torrico-Bascope, "Boost based on three-state switching cell for UPS applications," in Proc. Brazilian Power Electron. Conf., 2009, pp. 313–318

[10] Y. Jang and M. M. Jovanovic, "Interleaved boost converter with intrinsic voltage-doubler characteristic for universal-line PFC front end," IEEE Trans. Power Electron., vol. 22, no. 4, pp. 1394–l40l, Jul. 2007

[11] Y. Alcazar, D. de Souza Oliveira, F. Tofoli, and R. Torrico-Bascope, "DC-DC nonisolated boost converter based on the three-state switching cell and voltage multiplier cells," IEEE Trans. Power Electron., vol. 60, no. 10, pp. 4438–4449, Oct. 2013

[12] K. D. Kim, J. G. Kim, Y. C. Jung, and C. Y.Won, "Improved non-isolated high voltage gain boost converter using coupled inductors," in Proc. IEEE Int. Conf. Electric. Mach. Syst., Aug. 2011, pp. 20–23

[13] N. Vazquez and L. Estrada, “The tapped-inductor boost converter,” in Proc. IEEE Int. Symp. Ind. Electron., Jun. 2007, pp. 531–538

[14] T.-F. Wu, Y.-S. Lai, J.-C. Hung, and Y.-M. Chen, “Boost converter with coupled inductors and buck-boost type of active clamp,” IEEE Trans. Ind. Electron., vol. 55, no. 1, pp. 154–162, Jan. 2008

[15] A high voltage gain DC/DC converter for energy harvesting in single module photovoltaic applications," Industrial Electronics (ISIE), 2010 IEEE International Symposium on , vol., no., pp.550,555, 4-7 July 2010

[16] H. S. H. Chung, W. C. Chow, S. Y. R. Hui, and S. T. S. Lee, “Development of a switched-capacitor DC–DC converter with bidirectional power flow,” IEEE Trans. Circuits Syst. I, Fund. Theory Appl., vol. 47, no. 9, pp. 1383–1389, Sep. 2000

[17] B. Axelrod, Y. Berkovich, and A. Ioinovici, “Switched-capacitor /switched-inductor structures for getting transformerless hybrid DC–DC PWM converters,” IEEE Trans. Circuits Syst. I, vol. 55, no. 2, pp. 687–696, Mar. 2008

[18] L. S. Yang, T. J. Liang, H. C. Lee, and J. F. Chen, “Novel high step-up DC–DC converter with coupled-inductor and voltage-doubler circuits,” IEEE Trans. Ind. Electron., vol. 58, no. 9, pp. 4196–4206, Sep. 2011

[19] J. W. Baek, M. H. Ryoo, T. J. Kim, D. W. Yoo, and J. S. Kim, “High boost converter using voltage multiplier,” in Proc. IEEE the 39th Annu. Conf. IEEE Ind. Electron. Society, 2005, pp. 567–572

[20] L. Huber and M. M. Jovanovic, “A design approach for server power supplies for networking applications,” in Proc. IEEE INTELEC, 2000, pp. 1163–1169

[21] T. F. Wu and T. H. Yu, “Unified approach to developing single-stage power converters,” IEEE Trans. Aerosp. Electron. Syst., vol. 34, no. 1, pp. 211–223, Jan. 1998

[22] D. Maksimovic and S. Cuk, “Switching converters with wide dc conversion range,” IEEE Trans. Power Electron., vol. 6, no. 1, pp. 377–390, Jan. 1991